Fast Deblurring Method for Computed Tomography Medical Images Using a Novel Kernels Set

Zohair Al-Ameen[1], Ghazali Sulong[1] and Md. Gapar Md. Johar[2]

[1] *Faculty of Computer Science and Information Systems, Universiti Teknologi Malaysia (UTM), 81310 UTM Skudai, Johor, Malaysia*

[2] *Faculty of Information Sciences and Engineering, Management and Science University (MSU), 40100 MSU Shah Alam, Selangor, Malaysia*

zohair_alameen@yahoo.com, ghazali@spaceutm.edu.my, gapar@msu.edu.my.

Abstract

Medical images such as computed tomography (CT) are degraded by different types of blur due to the imperfect resolution of the imaging system, data loss at the acquisition time and other technical reasons. The fastest way to deblur an image is by convolving a special kernel to the corrupted image. Laplacian kernels are famous and widely used in this field, but the issue is only few kernels are presented. This paper is trying to simulate the blur problem using various types of blur and attempt to restore the degraded images by using twenty novel kernels. Moreover, these kernels were tested with five types of blur that are: Average, Box, Gaussian, Pillbox and Atmospheric turbulence blur to determine which type of blur is suitable to be employed with kernels the most. The accuracy of the experimental results is measured with five diverse methods along with the success and the failure ratios. Finally, these kernels are applied to naturally degraded images obtained from different CT imaging systems.

Keywords: *Computed Tomography (CT), Deblurring CT medical images, Sharpening kernels, Image deblurring, Average blur, Box blur, Gaussian blur, Pillbox blur, Atmospheric turbulence blur, Accuracy measurement methods*

1. Introduction

Digital images are matrixes of numbers employed to show vital information. The methods of capturing and recording these images are diverse; therefore, the probabilities of having errors or degradations throughout the procedure of capturing and recording images are also increased [1]. The degradations that affect an image are noise, contrast imperfections, and blur [2]. This paper handles the blur degradation only. Blurring is uneasy to evade in every imaging device [18]. Blurry images are formed by convolving the original images with the point-spread function (PSF) [19]. CT medical images are known to be affected by blur [22] [7] [9]. Blur degrades CT images by the reasons of Gaussian noise [3], employing a denoising procedure on the degraded image [4], imperfect resolution of the imaging system [7], losing information throughout the acquisition process [8], and employing low-pass filters for reducing noise leads to blur amplification [9]. Blur has diverse types such as, atmospheric turbulence [12], Average [15], Box [17], Gaussian [14], Pillbox blur [16], and so on. Image deblurring is an essential topic in the area of image processing. The deblurring process results in sharpened details, better image quality and visualization [19]. The image restoration is a vital phase to recover images from their degradations; these techniques are considered as direct techniques when the outcome is formed in a one-step mode. Consistently, it's considered as indirect techniques when the outcome is acquired with a number of iterations. Famous restoration methods such as Wiener Filtering and Richardson-Lucy are examples of direct and indirect methods. The problems with these techniques are the essential need for the point-spread function (PSF), and determining the sufficient iterations required to restore the image [15]. Therefore, the use of kernels is more suitable, because determining the PSF and/or the number of iteration is not required.

2. Deblurring Procedure

Using kernels to deblur images is very simple. The basic concept is to convolve the kernel with the blurry image to obtain a sharper image. It takes one mathematical operation only, and it's fast and reliable. Suppose the degraded image is (D), the kernel is (K), and the convolution process is (⊗), the restored image (R) can be described as the subsequent:

$$\mathbf{R = D \otimes K}$$

Laplacian kernels are well-known in the sharpening field. The problem is it contains only few sets of kernels. Therefore, the process of sharpening cannot be tuned well; the kernels either sharpen more or less than the desired amount. Thus, more sets of Kernels are demanded. This paper presents twenty novel kernels to tune and get the exact sharpening amount. The new kernels are:

0	-1	0
0	3	0
0	-1	0

K1

-1	0	-1
0	5	0
-1	0	-1

K2

-1	2	-1
0	1	0
-1	2	-1

K3

-1	0	-1
2	1	2
-1	0	-1

K4

-1	0	-1
-1	7	-1
-1	0	-1

K5

-1	-1	-1
0	7	0
-1	-1	-1

K6

-1	-1	-1
1	5	1
-1	-1	-1

K7

-1	1	-1
0	3	0
-1	1	-1

K8

0	-2	0
0	5	0
0	-2	0

K9

-2	0	-2
0	9	0
-2	0	-2

K10

0	-1	0
-1	5	-1
0	-1	0

K11

-1	0	-1
-2	9	-2
-1	0	-1

K12

-2	-1	-2
0	11	0
-2	-1	-2

K13

-1	-2	-1
0	9	0
-1	-2	-1

K14

-1	-2	-1
-1	11	-1
-1	-2	-1

K15

0	-2	0
-1	7	-1
0	-2	0

K16

0	0	0
-1	3	-1
0	0	0

K17

-2	0	-2
-1	11	-1
-2	0	-2

K18

0	-1	0
-2	7	-2
0	-1	0

K19

-2	0	-2
1	7	1
-2	0	-2

K20

Each of the above kernels has a different sharpening amount depending on the type of the blur and the blur volume. Using the correct kernel would grant the image a better and precise sharpening amount. Therefore, all the kernels would be tested with the five types of blur that are mentioned earlier, and the accuracy of the resulted image would be measured in different measurement techniques.

3. Accuracy Measurement Methods

Calculating the precision of the resulted image to the original one is considered as an important step. Therefore, traditional measuring techniques are utilized such as, Peak Signal to Noise Ratio (PSNR), Root Mean Square Error (RMSE), and Signal to Noise Ratio (SNR). PSNR computes the peak error. Reasonably, a greater rate of PSNR is better since it shows that the ratio of Signal to Noise is higher. In this method, the 'signal' is the reference image, and the 'noise' is the error in restoration [11]. Greater values for SNR and PSNR refer to a minor alteration between the original image and the restored image. The key benefit of these methods is its calculation simplicity. The Root Mean Square Error (RMSE) is the square root of the mean square error (MSE), lesser values of RMSE refers to a lower deference to the referenced image, and that leads to a better-quality image [5]. The equations of PSNR [6], SNR [5] and RMSE [5] are:

$$\mathrm{PSNR} = 20\log_{10}\frac{255}{\sqrt{MSE}}$$

$$\mathrm{SNR} = 10\log_{10}\frac{\sum_{i=1}^{n}\sum_{j=1}^{m}\left(\mathrm{A}_{ij}\right)^2}{\sum_{i=1}^{n}\sum_{j=1}^{m}\left(\mathrm{A}_{ij}-\mathrm{B}_{ij}\right)^2}$$

$$\mathrm{RMSE} = \sqrt{\mathrm{MSE}} = \sqrt{\frac{1}{\mathrm{MN}}\sum_{\mathrm{i=1}}^{\mathrm{n}}\sum_{\mathrm{j=1}}^{\mathrm{m}}\left(\mathrm{A(i,j)}-\mathrm{B(i,j)}\right)^2}$$

Where: (A) is the referenced image; (B) is the restored image; (MN) is the height and width of the image. Furthermore, another two methods were used to measure the accuracy of the resulted image, such as Improvement in Signal-to-Noise Ratio (ISNR) and Universal Image Quality Index (UIQI). The ISNR is usually employed to measure the quality of the image in any imaging device. It’s a powerful tool because it involves the reference image, the corrupted image and the restored image in the quality measurement process [20]. The equation of ISNR is [20]:

$$\mathrm{ISNR} = 10\log\frac{\mathrm{MSE}\ (\mathrm{S},\mathrm{C})}{\mathrm{MSE}\ \left(\mathrm{S},\hat{\mathrm{S}}\right)}$$

Where, (S) is the reference image, (C) is the corrupted image, ($\hat{\mathrm{S}}$) is the restored image. Similarly, the UIQI measurement of the quality between the reference and result images is separated into three diverse assessments: luminance, contrast, and structural comparisons [21]. The equation of UIQI is [21]:

$$\mathrm{UIQI} = \frac{4\ \mu_x\mu_y\ \sigma_{xy}}{\left(\mu_x^2+\mu_y^2\right)\left(\sigma_x^2+\sigma_y^2\right)}$$

Where, (σ_x^2) is the variance of (μ_x), (σ_y^2) is the variance of (μ_y), (σ_{xy}) is the covariance of (μ_x , μ_y), (μ_x) = {$x_1 \dots x_n$} and (μ_y) = {$y_1 \dots y_n$} [13].

4. Experimental Results

To determine which type of blur kernels can restore, an experiment has been conducted on five types of blur, namely are: Average, Box, Gaussian, Pillbox and Atmospheric turbulence blur. The degraded images of different types of blur are demonstrated in Figure 1. Consequently, the twenty kernels were applied to each type of blur. The accuracy was measured to recognize the restoration capability for every kernel and similarly to know which type of blur kernels can deblur the best. This paper will show only three results for each type of blur, and they are the worst, average and the finest result. The results of the experiment are illustrated in Figures 2, 3, 4, 5 and 6. The accuracy measurements along with the success and failure ratios are clarified in the subsequent tables.

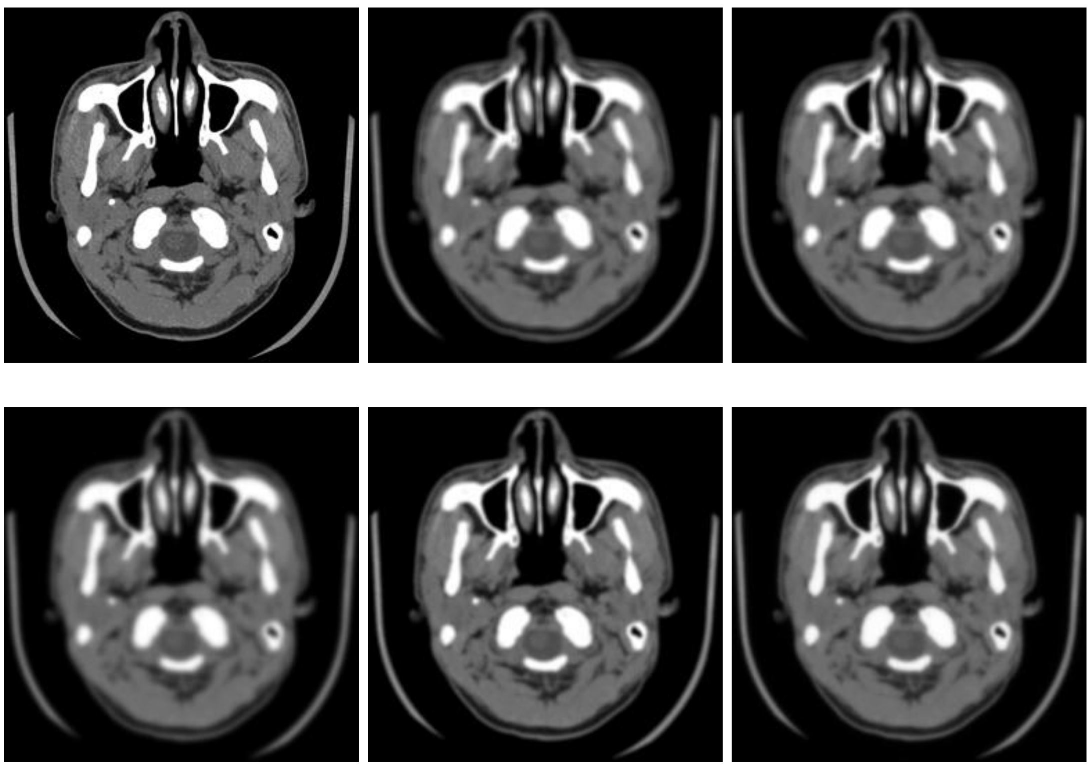

Figure 1. CT images from left to right, top to bottom: original image, image degraded by average blur [5x5] with PSNR (22.9296), image degraded by Box Blur R=2 with PSNR (22.9235), image degraded by Gaussian Blur R=2 with PSNR (21.7893), image degraded by Pillbox Blur R=2 with PSNR (25.6318), and image degraded by Atmospheric turbulence Blur k=0.002 with PSNR (23.8106)

Figure 2. (Average Blur Restoration) Images from left to right: The worst result by K18, the average result by K15, and the best result by K11

Figure 3. (Box Blur Restoration) Images from left to right: The worst result by K18, the average result by K20, and the best result by K11

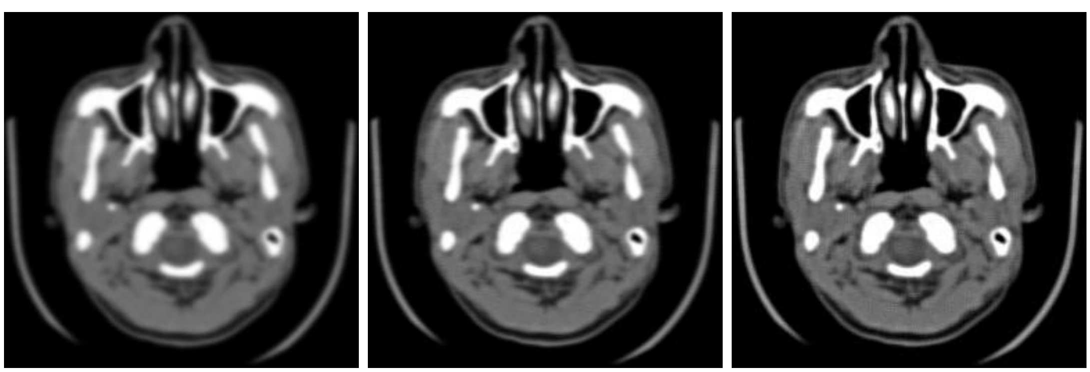

Figure 4. (Gaussian Blur Restoration) Images from left to right: The worst result by K1, the average result by K7, and the best result by K20

Figure 5. (Pillbox Blur Restoration) Images from left to right: The worst result by K18, the average result by K6, and the best result by K11

Figure 6. (Atmospheric Turbulence Blur Restoration) Images from left to right: The worst result by K18, the average result by K14, and the best result by K8

Table 1. The Accuracy Measurement with the Average Blur

Table 1	**K1**	**K2**	**K3**	**K4**	**K5**	**K6**	**K7**	**K8**	**K9**	**K10**
PSNR	23.2393	22.3520	22.6203	23.2125	20.7704	21.6838	22.7070	22.6925	23.0789	18.3453
SNR	12.2076	11.3203	11.5886	12.1809	9.7388	10.6522	11.6754	11.6608	12.0473	7.3137
RMSE	0.0689	0.0763	0.0740	0.0691	0.0915	0.0824	0.0732	0.0733	0.0702	0.1210
ISNR	-0.3096	0.5777	0.3094	-0.2829	2.1592	1.2458	0.2226	0.2372	-0.1493	4.5843
UIQI	0.6734	0.6506	0.6592	0.6658	0.6221	0.6315	0.6502	0.6611	0.6688	0.5670

K11	**K12**	**K13**	**K14**	**K15**	**K16**	**K17**	**K18**	**K19**	**K20**	
23.3943	19.1059	17.7151	20.8183	19.4744	23.0285	23.2756	16.9594	22.3912	19.7919	*Average Blur Filter Size [5x5]*
12.3626	8.0743	6.6835	9.7866	8.4428	11.9968	12.2440	5.9278	11.3596	8.7603	
0.0677	0.1108	0.1301	0.0910	0.1062	0.0706	0.0686	0.1419	0.0759	0.1024	
-0.4646	3.8237	5.2145	2.1114	3.4552	-0.0988	-0.3460	5.9702	0.5384	3.1377	
0.6678	0.5906	0.5492	0.6099	0.5844	0.6581	0.6706	0.5403	0.6518	0.5944	

Table 2. The Accuracy Measurement with the Box Blur

Table 2	**K1**	**K2**	**K3**	**K4**	**K5**	**K6**	**K7**	**K8**	**K9**	**K10**
PSNR	23.2952	22.6155	22.7237	23.3338	21.1367	22.1038	23.0426	22.8377	23.3015	18.8177
SNR	12.2636	11.5838	11.6920	12.3022	10.1051	11.0722	12.0110	11.8061	12.2699	7.7861
RMSE	0.0684	0.0740	0.0731	0.0681	0.0877	0.0785	0.0704	0.0721	0.0684	0.1146
ISNR	-0.3717	0.3080	0.1998	-0.4103	1.7868	0.8197	-0.1191	0.0858	-0.3780	4.1058
UIQI	0.7043	0.6872	0.6931	0.7001	0.6626	0.6723	0.6898	0.6962	0.7044	0.6127

K11	**K12**	**K13**	**K14**	**K15**	**K16**	**K17**	**K18**	**K19**	**K20**	
23.5467	19.5386	18.2633	21.3926	20.0720	23.3809	23.3175	17.4440	22.7098	20.2472	*Box Blur R=2*
12.5151	8.5070	7.2317	10.3610	9.0403	12.3492	12.2858	6.4123	11.6782	9.2156	
0.0665	0.1055	0.1221	0.0852	0.0992	0.0678	0.0683	0.1342	0.0732	0.0972	
-0.6232	3.3849	4.6602	1.5309	2.8516	-0.4573	-0.3939	5.4796	0.2137	2.6763	
0.7060	0.6353	0.5973	0.6551	0.6322	0.7004	0.7019	0.5884	0.6933	0.6377	

Table 3. The Accuracy Measurement with the Gaussian Blur

Table 3	K1	K2	K3	K4	K5	K6	K7	K8	K9	K10
PSNR	22.2999	25.3268	24.0202	22.6349	26.1804	25.7020	24.4101	24.7403	22.7286	26.2791
SNR	11.2683	14.2951	12.9885	11.6032	15.1487	14.6704	13.3784	13.7086	11.6969	15.2475
RMSE	0.0767	0.0542	0.0629	0.0738	0.0491	0.0519	0.0602	0.0579	0.0730	0.0485
ISNR	-0.5107	-3.5375	-2.2309	-0.8456	-4.3911	-3.9127	-2.6208	-2.9510	-0.9393	-4.4898
UIQI	0.6660	0.7274	0.6916	0.6756	0.7361	0.7344	0.7157	0.7120	0.6845	0.7283

K11	K12	K13	K14	K15	K16	K17	K18	K19	K20	
23.6244	26.2399	25.8424	25.8024	26.4414	24.1239	23.0159	25.3188	24.8368	26.4529	*Gaussian Blur R=2*
12.5928	15.2083	14.8108	14.7707	15.4098	13.0923	11.9842	14.2872	13.8051	15.4212	
0.0659	0.0488	0.0510	0.0513	0.0476	0.0622	0.0707	0.0542	0.0573	0.0476	
-1.8351	-4.4507	-4.0531	-4.0131	-4.6521	-2.3346	-1.2266	-3.5295	-3.0475	-4.6636	
0.6922	0.7289	0.7202	0.7321	0.7334	0.7080	0.6735	0.7142	0.7158	0.7368	

Table 4. The Accuracy Measurement with the Pillbox Blur

Table 4	K1	K2	K3	K4	K5	K6	K7	K8	K9	K10
PSNR	26.4307	23.6539	25.0098	25.7808	20.6342	21.9598	24.0466	24.8942	25.5266	16.8999
SNR	15.3991	12.6223	13.9782	14.7492	9.6026	10.9282	13.0149	13.8626	14.4950	5.8682
RMSE	0.0477	0.0657	0.0562	0.0514	0.0930	0.0798	0.0628	0.0569	0.0529	0.1429
ISNR	-0.7990	1.9779	0.6219	-0.1491	4.9976	3.6720	1.5852	0.7376	0.1052	8.7319
UIQI	0.7562	0.6932	0.7215	0.7345	0.6494	0.6631	0.6989	0.7179	0.7358	0.5749

K11	K12	K13	K14	K15	K16	K17	K18	K19	K20	
27.2989	18.1527	16.0221	20.2636	18.3563	25.4993	27.2304	15.2404	24.2244	18.7791	*Pillbox Blur R=2*
16.2673	7.1210	4.9905	9.2320	7.3246	14.4676	16.1988	4.2088	13.1928	7.7474	
0.0432	0.1237	0.1581	0.0970	0.1208	0.0531	0.0435	0.1730	0.0615	0.1151	
-1.6671	7.4791	9.6097	5.3682	7.2755	0.1325	-1.5986	10.3914	1.4074	6.8527	
0.7460	0.6080	0.5527	0.6327	0.5970	0.7167	0.7561	0.5434	0.7033	0.6091	

Table 5. The Accuracy Measurement with the Atmospheric Turbulence Blur

Table 5	K1	K2	K3	K4	K5	K6	K7	K8	K9	K10
PSNR	24.7109	27.0167	26.3800	24.9053	24.5671	25.6063	26.1963	27.3565	24.9290	20.6316
SNR	13.6793	15.9850	15.3483	13.8736	13.5355	14.5746	15.1647	16.3248	13.8973	9.6000
RMSE	0.0581	0.0446	0.0480	0.0569	0.0591	0.0524	0.0490	0.0429	0.0567	0.0930
ISNR	-0.9003	-3.2060	-2.5693	-1.0946	-0.7565	-1.7956	-2.3857	-3.5458	-1.1183	3.1790
UIQI	0.6926	0.7028	0.6980	0.6909	0.6694	0.6797	0.6927	0.7106	0.6943	0.6054

K11	K12	K13	K14	K15	K16	K17	K18	K19	K20	
26.9675	21.9256	19.6058	23.8448	22.1068	26.7636	25.9745	18.7646	26.8626	22.6590	*Atmospheric Turbulence Blur k=0.002*
15.9359	10.8939	8.5741	12.8132	11.0752	15.7320	14.9429	7.7330	15.8309	11.6273	
0.0448	0.0801	0.1046	0.0642	0.0785	0.0459	0.0503	0.1153	0.0454	0.0736	
-3.1568	1.8851	4.2049	-0.0342	1.7038	-2.9530	-2.1639	5.0460	-3.0519	1.1517	
0.7076	0.6329	0.5843	0.6535	0.6247	0.7018	0.6988	0.5749	0.7005	0.6366	

After measuring the accuracy, the success and failure ratios should be determined depending on the results illustrated in the above tables. The ratio will be computed depending on PSNR results, and it must be calculated for each blur category to identify the type of blur that can be restored efficiently using kernels. The ratios can be determined as the subsequent:

$$Success\ ratio = \frac{SK}{TNK} * 100\%$$

$$Failure\ ratio = \frac{FK}{TNK} * 100\%$$

Where, (SK) represents the number of kernels that scored a higher PSNR value than the PSNR value of the corresponding blurry image in Figure 1. (FK) represents the number of kernels that scored lower or equal PSNR values. (TNK) represents the total number of kernels. The success and failure ratios are illustrated in the subsequent table.

Table 6. The Success and Failure Ratios According to PSNR Statistics

Blur Type	*SK*	*FK*	*TNK*	*Success ratio %*	*Failure ratio %*
Average	6	14	20	30%	70%
Box	7	13	20	35%	65%
Gaussian	20	0	20	100%	0%
Pillbox	4	16	20	20%	80%
Atmospheric Turbulence	14	6	20	70%	30%
Overall Success Ratio	**51%**		***Overall Failure Ratio***		**49%**

5. Discussion

This paper proves lots of new concepts that they are: all the mentioned five types of blur can be restored using kernels but with diverse ratios depending on the type of blur and the blur density. Table 6 proves that the total success ratio is 51% of kernels to sharpen five types of blur. Furthermore, the behavior of the average and box blur is nearly the same. This inference has been inspired by comparing the results of the accuracy measurement techniques and the success and failure ratios between the two types of blur. Besides, the lowest ratio of success can be seen in the Pillbox blur, but still it has a reasonably high PSNR value among the restored images in the five types of blur, and that leads to a fact that the Pillbox blur can be restored efficiently but with certain types of kernels only. However, the atmospheric turbulence blur shows promising results to be deblurred with kernels when it gave a 70% succession ratio, and it gave the uppermost PSNR with the lowest RMSE values and that point to a fact that this type of blur can be restored efficiently but with precise type of kernels only. Lastly, the Gaussian blur is the most suitable type of blur to be restored with kernels due to its succession ratio that gave a 100% with 0% failure.

6. Applying Kernels to Naturally Degraded CT Images

In this section, several naturally degraded CT images were selected to be restored using the proposed kernels. Figures 7, 8, 9, and 10 illustrate the CT images and their restored versions.

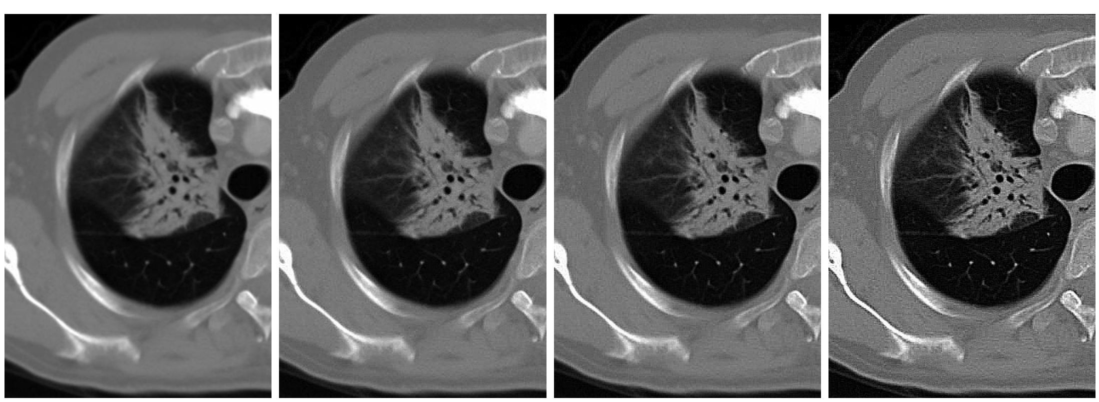

Figure 7. Images From left to right: original image, restored by K11, restored by K2, restored by K13

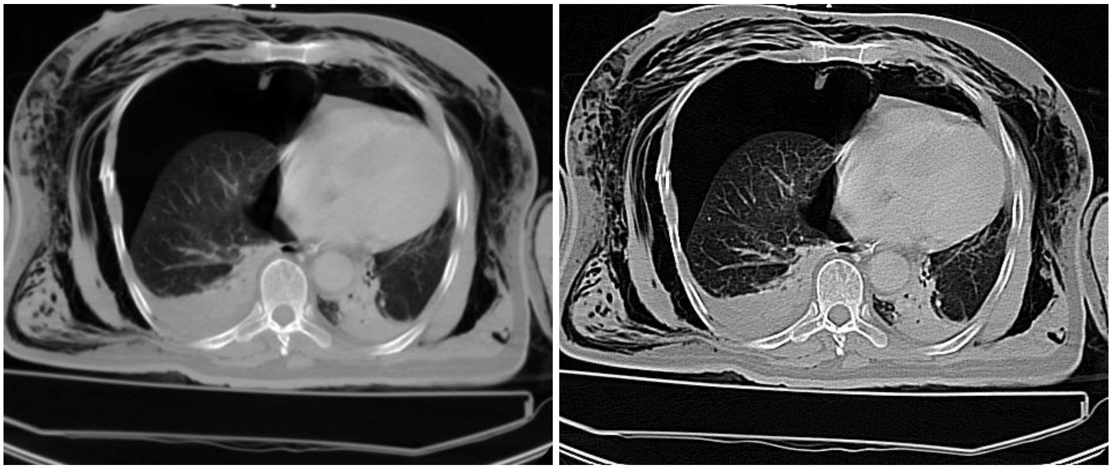

Figure 8. Images from left to right: original image, restored by K20

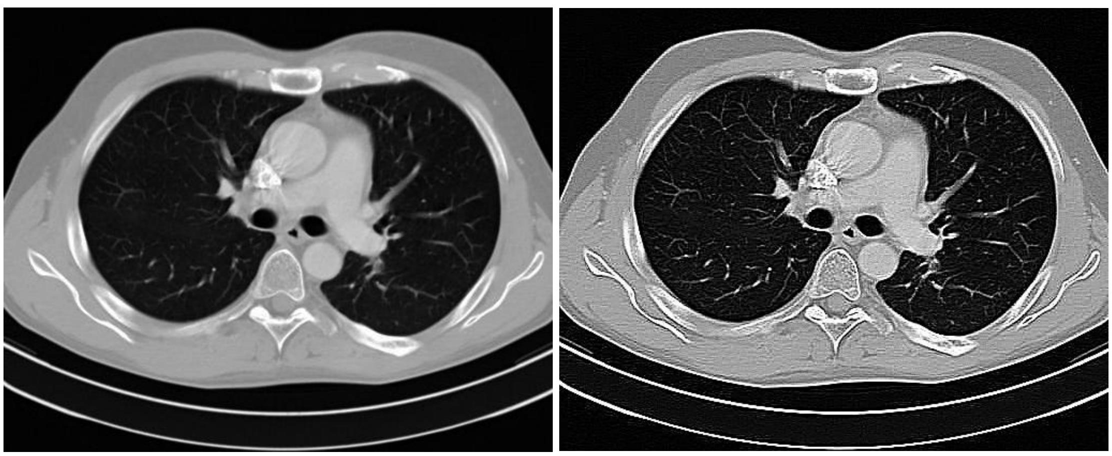

Figure 9. Images from left to right: original image, restored by K14

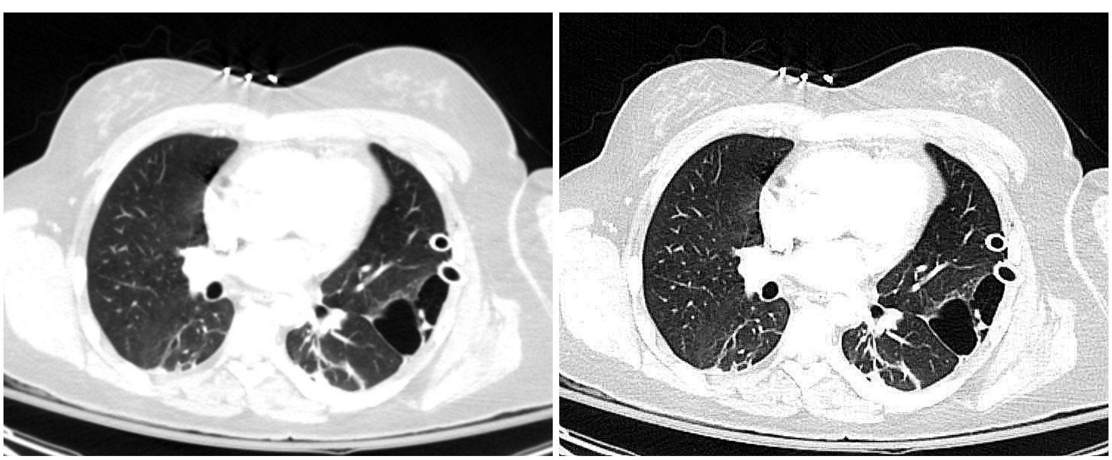

Figure 10. Images from left to right: original image, restored by K18

7. Conclusion

In ending words, kernels are the fastest way to restore blurry images, because only one mathematical operation is involved and no prior knowledge about the PSF is required. Furthermore, kernels can successfully restore the mentioned five types of blur. Likewise, the finest restored images by kernels are images blurred with atmospheric turbulence and Pillbox blur, although the fact that these types of blur have relatively large failure ratios, especially the Pill box blur. The best type of blur that can be used with kernels is the Gaussian blur because of its 100% success ratio. Moreover, the average blur and the Box blur have a reasonably similar behavior due to the converged results between them. As a final point, if the CT medical images are degraded with one of five types of blur mentioned earlier, they can be restored by utilizing the novel kernels set presented in this paper.

References

[1] S. W. Perry, H. S. Wong and L. Guan, Editors, "Adaptive Image Processing: A Computational Intelligence Perspective", (1st edition), CRC Press LLC, Boca Raton, Florida, **(2002)**.

[2] R. L. Lagendijk and J. Biemond, In: The Essential Guide to Image Processing, Edited A. C. Bovik, Academic Press, United States of America, **(2009)**.

[3] D. Palumbo, B. Yee, P. O'Dea, S. Leedy, S. Viswanath and A. Madabhushi, Editors, "Interplay between Bias Field Correction, Intensity Standardization, and Noise Filtering for T2-weighted MRI", Annual International Conference of the IEEE Engineering in Medicine and Biology Society (EMBC), **(2011)** August 30-September 3; Boston, MA, USA.

[4] X. Yan, M. Zhou, L. Xu, W. Liu and G. Yang, Editors, "Noise Removal of MRI data with Edge Enhancing", 5th International Conference on Bioinformatics and Biomedical Engineering (iCBBE), **(2011)** May 10-12; Wuhan, China.

[5] A. K. Hmood, Z. M. Kasirun, H. A. Jalab, G. M. Alam, A. A. Zaidan and B. B. Zaidan, "On the accuracy of hiding information metrics: Counterfeit protection for education and important certificates", International Journal of the Physical Sciences, vol. 5, no. 7, **(2010)**, pp. 1054-1062.

[6] C. Wee, R. Paramesran and R. Mukundan, Editors, "Quality assessment of Gaussian blurred images using symmetric geometric moments", 14th international conference on image analysis and processing (ICIAP), **(2007)** September 10-14; Modena, Italy.

[7] M. N. Hussien and M. I. Saripan, Editors, "Computed Tomography Soft Tissue Restoration using Wiener Filter", IEEE Student Conference on Research and Development (SCOReD), **(2010)** December 13-14; Putrajaya, Malaysia.

[8] S. Goliaei and S. Ghorshi, Editors, "Tomographical Medical Image Reconstruction Using Kalman Filter Technique", Ninth IEEE International Symposium on Parallel and Distributed Processing with Applications Workshops (ISPAW), **(2011)** May 26-28; Busan, South Korea.

[9] F. Attivissimo, G. Cavone, A. M. L. Lanzolla and M. Spadavecchia, "A Technique to Improve the Image Quality in Computer Tomography", IEEE Transactions on Instrumentation and Measurement, vol. 59, no. 5, **(2010)**, pp. 1251 - 1257.

[10] S. Poobal and G. Ravindran, "The Performance of Fractal Image Comparison on Different Imaging Modalities Using Objective Quality Measures", International Journal of Engineering Science and Technology (IJEST), vol. 3, no. 1, **(2011)**.

[11] S. D. Desai and L. Kulkarni, "A Quantitative Comparative Study of Analytical and Iterative Reconstruction Techniques", International Journal of Image Processing (IJIP), vol. 4, no. 4, **(2010)**.

[12] Z. Xiang and P. Milanfar, Editors, "Stabilizing and deblurring atmospheric turbulence", IEEE International Conference on Computational Photography (ICCP), **(2011)** April 8-10; Pittsburgh, USA.

[13] E. Blasch, X. Li, G. Chen and W. Li, Editors, "Image quality assessment for performance evaluation of image fusion", IEEE 11th International Conference on Information Fusion, **(2008)** June 30-July 3; Cologne, Germany.

[14] Y. Lai, C. Huo, Y. Yu and T. Sun, Editors, "PSO-based estimation for Gaussian blur in blind image deconvolution problem", IEEE International Conference on Fuzzy Systems (FUZZ), **(2011)** June 27-30; Taipei, Taiwan.

[15] S. S. Al-amri and N. V. Kalyankar, "A Comparative Study for Deblurred Average Blurred Images", International Journal on Computer Science and Engineering (IJCSE), vol. 2, no. 3, **(2010)**.
[16] S. Chardon, B. Vozel and K. Chehdi, Editors, "A comparative study between parametric blur estimation methods", IEEE International Conference on Acoustics, Speech, and Signal Processing, **(1999)** March 15-19; Phoenix, USA.
[17] A. Lukin, Editor, "Tips and tricks: Fast image filtering algorithms. Proceedings of Graphicon", **(2007)** June 23-27; Moscow, Russia.
[18] M. V. Nayakkankuppam and Y. V. Venkatesh, "Deblurring the Gaussian blur using a wavelet transform", Pattern Recogn., vol. 28, no. 7, **(1995)**, pp. 965–976.
[19] S. L. Kala, Editor, "Deblurring Images via Partial Differential Equations", Proceedings of the Louisiana-Mississippi Section of the Mathematical Association of America, **(2004)**; Mississippi, USA.
[20] P. F. Meza, E. M. Vera, S. N. Torres and S. E. Godoy, Editors, "A new Reference-Free Infrared Image Quality Metric for Nonuniformity Correction", Proceedings of the 14th World Multi-Conference on Systemics, Cybernetics and Informatics: WMSCI, **(2010)** June 29 - July 2; Orlando, USA.
[21] A. Bouzerdoum, A. Havstad and A. Beghdadi, Editors, "Image quality assessment using a neural network approach", Proceedings of the Fourth IEEE International Symposium on Signal Processing and Information Technology, **(2004)** December 18-21, pp. 330-333.
[22] E. Rollano-Hijarrubia, R. Manniesing and W. J. Niessen, "Selective Deblurring for Improved Calcification Visualization and Quantification in Carotid CT Angiography: Validation Using Micro-CT", IEEE Transactions on Medical Imaging, vol. 28, no. 3, **(2009)**.

Authors

Zohair Al-Ameen was born in the United Kingdom in 1985, obtained his B.Sc. degree in Computer Science from the University of Mosul - IRAQ in 2008. In 2011 he obtained his M.Sc. in Computer Science from Universiti Teknologi Malaysia (UTM). His research interests include Image and Video Processing, Image Restoration, Image Enhancement, Medical Imaging, Segmentation, Optical Characters Recognition, Motion Detection, and Pattern Recognition. Currently he is pursuing his Ph.D. in computer science in the field of Medical Imaging in terms of Enhancement and Restoration.

Prof. Dr. Ghazali Sulong was born in 1958. He graduated with M.Sc. and Ph.D. in computing from University of Wales, United Kingdom in 1982 and 1989 respectively. His academic career has begun since 1982 at Universiti Teknologi Malaysia (UTM). Later in 1999, he was promoted as a full Professor of Image Processing and Pattern Recognition. He has authored/co-authored of more than 50 technical papers for journals, conference proceedings and book chapters. His research area includes Image and Video Processing, Pattern Recognition, Watermarking and Steganography.

Prof. Dr. Md. Gapar Md. Johar A certified e-commerce consultant, he has over 30 years working experience in software and application development. His research interests include object-oriented analysis and design, software engineering, Java programming, digital image processing, Radio Frequency Identification (RFID) and knowledge management. Currently he is the vice president academic for Management and Science University (MSU). Md Gapar holds BSc (Hons) in Computer Science, MSc in Data Engineering and PhD in Computer Science.